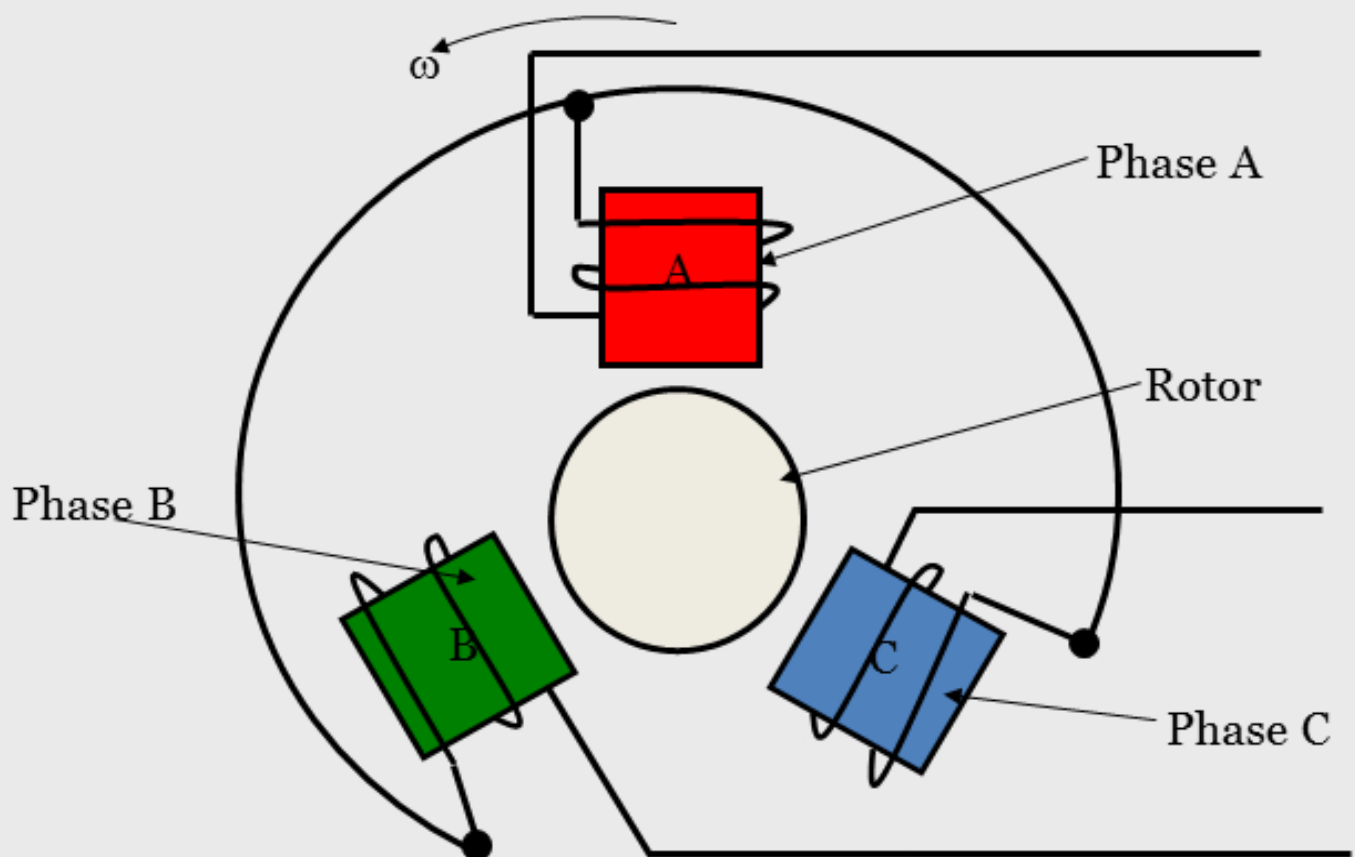


Principles of Electrical Machinery

Dr. Praveen Kumar



DESHYA
Technologies Pvt Ltd

Preface

The primary objective of this book is to develop foundation in the fundamental principles of electric machinery. The book concentrates on the principles of electromechanical energy conversion and its application to electric machinery. An effort is made to develop the theory of operation of machines from electromechanical energy conversion viewpoint. Generally, the operation of electrical machines is better understood using electromagnetic and the analysis of the machine is easier to perform using electrical equivalent circuit. In this book a link between the electromagnetic viewpoint and the equivalent circuit is developed. This link is developed using the principles of electromechanical energy conversion (EMEC).

The chapters 1 and 2 of the book deal with the basics of electric circuits and magnetic circuits. In chapter 3 the principles of EMEC is introduced and its application to singly excited systems is explained. The chapter 4 deals with the electromechanical energy conversion for doubly excited system. Based the principles of EMEC the electrical equivalent circuits of a.c. machines is derived. The common underlying principles of electrical machines are also presented in chapter 4. The chapter 5 explains the working principles of electrical machines and explains the phenomena of rotating magnetic fields and torque production in a.c. machines. The chapters 6 and 7 are dedicated to principles of induction machines and their speed control. The chapter 8 deals with synchronous generators and motor.

The unique feature of this book is extensive use of figures and animations to explain the phenomena occurring in electrical machines. Besides the animations, elaborate explanation of phenomenon is given boxes. The boxes are used ensure that the flow of the text in the book remains intact. Since the book is in electronic format, it helps the reader to navigate through the animations, figures, boxes, etc. in a simple and efficient manner.

It was our endeavour to write and publish an accurate book. However, it is possible that there may still be some typological and numerical errors in the book. It is very likely that the readers might feel that some sections need better explanation. We welcome any comments and suggestions in this regard and will consider them for future revisions.

Copyrights

Preface

Table of Content

Chapter 1: Fundamentals of Electrical Circuits

1.1. Introduction

1.2. Phasor Representation of Sinusoids

Figure 1.1: Reconstruction of sine and cosine waves from phasor.

Animation 1.1: Phasor Representation of Sinusoidal quantities.

Figure 1.2a: Phasor representation of the currents.

Figure 1.2b: The waveforms of currents.

1.3. Multiplication and Division of Complex Quantities

1.4. Power and Roots of Complex Quantities

1.4.1. Complex Power

Figure 1.3: The impedance Z consumes complex power.

1.4.2. Summary of Complex Power

Example 1.1

Figure 1.4: Series R-L-C network.

Figure 1.5: The phasor diagram of the R-L-C network.

Example 1.2

1.5. Network Theorems for Sinusoidal Steady State Analysis

1.5.1. Steps to Analyze AC Circuits

1.5.2. Nodal Analysis

Figure 1.6: Network for Nodal Analysis.

Figure 1.7a: Frequency domain equivalent of the circuit in figure 1.6.

Figure 1.7b: The network for nodal analysis.

1.5.3. Mesh Analysis

1.5.4. Superposition Theorem

Figure 1.8: The network to illustrate superposition theorem.

Figure 1.9a: Equivalent circuit with just the *DC* voltage source.

Figure 1.9b: Equivalent circuit with just the *DC* voltage source.

Figure 1.9c: Equivalent circuit with just the current source.

1.5.5. Thevenin and Norton Equivalent Circuits (figure 1.10)

Figure 1.10: The Network for Thevenin and Norton's Theorem.

Figure 1.11a: The Network for Thevenin Theorem for finding Z_{th} .

Figure 1.11b: The Network for Thevenin Theorem for finding V_{th} .

Figure 1.12: The Network for Example 1.3.

Figure 1.13: Location of supernode for the network shown in figure 1.12.

Example 1.3

1.6. Three Phase Circuits

1.6.1. Introduction

Figure 1.14a: Single phase 2 wire system.

Figure 1.14b: Single phase 3 wire system.

1.6.2. Transmission Systems

Figure 1.15: Two phase three wire system.

Figure 1.16: Three phase four wire system.

Figure 1.17: Three phase voltages.

1.6.3. Two and Three Phase System

1.6.3.1. Why Three Phase System?

1.6.3.2. Balanced Three Phase Voltages

Figure 1.18: A three phase generator.

1.6.3.3. Balanced Three Phase Systems

Figure 1.19a: Y connection of three phase source.

Figure 1.19b: Delta connection of three phase source.

1.6.3.4. Y and Delta Connections

Figure 1.20a: *abc* or positive sequence.

Figure 1.20b: *acb* or negative sequence.

1.6.4. Three Phase Loads

1.6.4.1. Balanced Three Phase Load

Figure 1.21a: Y connected three phase loads.

Figure 1.21b: Delta connected three phase loads.

1.6.4.2. Y or Delta Connected Load

1.6.4.3. Balanced Y-Y Connection

Figure 1.22: A balanced Y-Y system showing the source, line and load impedance.

Figure 1.23a: Phasor sum.

Figure 1.23b: Phasor sum of three line voltages.

Figure 1.24: Balanced Y-Y Connection.

Example 1.4

1.7. Balanced Y-Delta Connection

Figure 1.25: Balanced Y-Delta Connection.

1.7.1. Balanced Delta-Delta Connection

Figure 1.26: Balanced Delta-Delta Connection.

1.7.2. Balanced Delta-Y Connection

Figure 1.27: A balanced Delta-Y connection.

Example 1.5

Example 1.6

1.8 Summary

Chapter 2: Principles of Magnetic Circuits

2.1. Introduction

2.2. Introduction to Magnetic Circuits

2.3. Simplifying Assumptions

2.3.1. Maxwell's Equation

2.3.2. Simplifying Assumptions (Magnetic Circuit)

2.4. Schematic of a Magnetic Circuit

Figure 2.1: Ferromagnetic core excited by a current source.

2.5. Definitions

2.5.1. Magnetomotive Force (MMF)

2.5.2. Magnetic Field Intensity (H)

2.5.3. Flux Density

2.5.4. Permeability

2.6. Reluctance and the Magnetic Circuit Equations

Example 2.1

2.7. Relative Permeability

Example 2.2

2.8. Analogies between Electric and Magnetic Circuits

Figure 2.2: Doughnut core with different ferromagnetic materials.

Figure 2.3: Doughnut core with different ferromagnetic materials and air-gap.

Example 2.3

2.9. Magnetic Circuits, Flux Linkages, Inductance and Energy

2.9.1. Materials and their Properties

2.9.2. Classification of Materials

2.10. Typical B vs. H curves for Ferromagnetic Materials

Figure 2.4: Magnetization curve of a ferromagnetic material.

Figure 2.5: Domains in an unmagnetized material.

2.10.1. Explanation of B vs. H Curve

2.10.2. Permeability

Figure 2.6: Permeability curve.

2.10.3. Practical B vs. H values and Curves

Figure 2.7: Typical B-H curve of a ferromagnetic material.

Table 2.1: Practical B vs. H values.

2.11. Hysteresis Loop

Figure 2.8: The hysteresis phenomenon is a ferromagnetic material when exposed to sinusoidal H .

Animation 2.1: Hysteresis loop in a ferromagnetic material excited by sinusoidal current.

Figure 2.9: The hysteresis curve.

2.11.1. Hysteresis Losses

Figure 2.10: The first half of the hysteresis curve.

Figure 2.11: The second half of hysteresis curve.

2.11.2. Eddy current losses

2.12. Summary

Chapter 3: Principles of Electromechanical Energy Conversion

3.1. Introduction

3.2. The Law of Conservation of Energy

Figure 3.1a: A simple resistive network.

Figure 3.1b: Force acting on a slab.

Figure 3.2: Schematic of EMEC system.

3.3. Conservation of Energy Applied to Systems with No Motion

Figure 3.3: Energy conversion system with no motion.

Figure 3.4: Change in current due to decrease in resistance.

Figure 3.5: Power variation due to change in resistance.

Figure 3.6: Change in current due to increase in resistance.

Figure 3.7: Change in power due to increase in resistance.

Box 3.1

Figure 3.8: Change in stored energy with change in resistance.

3.4. Conservation of Energy Applied to Systems with Motion

Figure 3.9: EMEC system with motion.

Figure 3.10a: Initial position of the plunger.

Figure 3.10b: Final position of the plunger.

Figure 3.11: Flux linkage versus current curve.

3.4.1. Slow Movement

Figure 3.12: Change in inductance with respect to plunger position.

Figure 3.13: Variation of flux linkage with respect to current for different positions of plunger.

Figure 3.14: Field energy stored in the system.

Figure 3.15: Three dimensional view of the ferromagnetic core.

Example 3.1

Figure 3.E1.1: Figure for example 3.1.

Figure 3.E1.2: Flux lines for the initial position of the plunger.

Figure 3.E1.3: 3D section of the plunger. The flux lines enter perpendicular to the face of the plunger.

Figure 3.E1.4: Flux lines for the final position of the plunger.

Figure 3.E1.5: Variation of inductance with plunger position.

Figure 3.E1.6: Flux linkage versus current curve.

3.4.2. Instantaneous Movement

Figure 3.16: Variation of flux linkage in case of slow motion of plunger.

3.4.3. Transient Movement

Figure 3.17: Variation of flux linkage in case of transient motion of plunger.

3.5. Force acting on the Moving System Using Energy

Figure 3.18: Variation of flux linkage for incremental motion of plunger.

Box 3.2

Example 3.2

Figure 3.E2.1: Force versus plunger position curve.

Figure 3.E2.2: Force calculation using equation 3.26.

Figure 3.E2.3: Difference in force calculation using equation 3.26 and 3.48

Box 3.3

Figure 3.B3.1a: Force versus plunger position for slow motion.

Figure 3.B3.1b: Force versus plunger position for fast motion.

Figure 3.B3.1c: Force versus plunger position for very fast motion.

Figure 3.B3.2a: Deviation for slow motion.

Figure 3.B3.2b: Deviation for fast motion.

Figure 3.B3.2c: Deviation for very fast motion.

3.6. Force acting on the Moving System Using Co-Energy

Figure 3.19: Non-linear B-H curve for a ferromagnetic material.

Figure 3.20: Linear B-H curve for a ferromagnetic material.

Box 3.4

3.7. Torque acting on Rotating Systems

Figure 3.21: Rotating electromechanical energy conversion system.

Figure 3.22a: a-axis of the rotor is coincident with the d-axis. This is minimum reluctance position of rotor.

Figure 3.22b: b-axis of the rotor is coincident with the d-axis. This is maximum reluctance position of rotor.

Figure 3.23: Variation of reluctance with change in rotor position.

Animation 3.1: Variation of reluctance with rotor position in a singly excited system.

Figure 3.24: Average torque as a function of load angle.

3.8. Summary

Chapter 4: Electromechanical Energy Conversions in Doubly Excited Systems

4.1. Introduction

4.2. Doubly Excited Magnetic Systems

4.2.1. Doubly excited EMEC System with Linear Motion

Figure 4.1: Doubly excited electromechanical energy conversion system.

Figure 4.2: Path of integration for determining the stored field energy in doubly excited electromechanical energy conversion system.

4.2.2. Doubly excited EMEC System with Rotational Motion

Figure 4.3: Doubly excited rotational electromechanical energy conversion system.

Animation 4.1: The flux is produced by stator and rotor currents. These flux lines see a varying reluctance as the rotor moves.

4.2.3. Analysis of Torque Produced by doubly excited EMEC System

Animation 4.2: Variation of reluctance with rotor position in a doubly excited system.

Figure 4.4: Variation of reluctance with change in rotor position for doubly excited rotational electromechanical energy conversion system.

Animation 4.3: The flux is produced by stator current. These flux lines see a varying reluctance as the rotor moves.

Animation 4.4: The flux is produced by rotor current. These flux lines see a varying reluctance as the rotor moves.

Figure 4.5: Doubly excited rotational electromechanical energy conversion system with cylindrical rotor.

Animation 4.5: Variation of reactance in a cylindrical rotor actuator.

Animation 4.6: The flux is produced by stator current. These flux lines see a constant reluctance as the rotor moves.

Figure 4.6: Doubly excited rotational electromechanical energy conversion system with cylindrical stator and salient pole rotor.

Animation 4.7: Variation of reactance in a salient pole rotor motor with two poles.

Animation 4.8: The flux is produced by current in stator coil and its variation with rotor position.

Animation 4.9: The flux is produced by current in rotor coil and its variation with rotor position.

Animation 4.10: The flux is produced by current in stator and rotor coils and its variation with rotor position.

Figure 4.7: Doubly excited rotational electromechanical energy conversion system with cylindrical stator and cylindrical rotor.

Animation 4.11: Variation of mutual inductance in a single phase machine.

Animation 4.12: The flux is produced by stator and rotor current.

Animation 4.13: The flux lines due to current in stator coil.

Animation 4.14: The flux lines due to current in the rotor coil.

4.3. Single Phase Non-Salient Machine

Figure 4.8: Single phase non salient pole motor.

Figure 4.9: Variation of mutual inductance with change in rotor position.

Animation 4.15: Flux linked by rotor coils in a two phase machine.

Box 4.1

Figure 4.B1.1: Single phase motor with stator coil excited by a DC source.

Figure 4.B1.2: Flux lines in produced by direct current in the stator coil.

Figure 4.B1.3a: Position of the rotor coil when the rotor has moved by 90 degrees mechanically.

Figure 4.B1.3b: Position of the rotor coil when the rotor has moved by 135 degrees mechanically.

Figure 4.B1.3c: Position of the rotor coil when the rotor has moved by 180 degrees mechanically.

Figure 4.B1.4: Flux linked by rotor coil with change is rotor position.

4.4. Two Phase Non-Salient Machine

Figure 4.10: Two phase non salient pole motor.

Figure 4.11: Variation of mutual inductance in two phase non salient pole motor.

Animation 4.16: Flux linked in two phase machine.

Box 4.2

Figure 4.B2.1: Two phase cylindrical rotor motor.

Figure 4.B2.2a: Flux seen by rotor coils at the initial position.

Figure 4.B2.2b: Flux seen by rotor coils when the rotor moves by 45 degrees mechanically.

Figure 4.B2.3: Flux linked by rotor coils due to excitation of phase A of stator.

Figure 4.B2.4: Flux seen by rotor coils when the phase B of the stator is excited by direct current.

Figure 4.B2.5: Flux linked by rotor coils due to excitation of phase A of stator.

4.5. Two Phase Non-Salient Synchronous Machine

Box 4.3

Figure 4.B3.1: Equivalent circuit of a synchronous machine.

Figure 4.B3.2a: Phasor diagram of a synchronous machine for $\delta > 0$.

Figure 4.B3.2b: Phasor diagram of a synchronous machine for $\delta < 0$.

4.6. Two Phase Non-Salient Induction Machine

Box 4.4

Figure 4.B4.1: Equivalent circuit for equation B4.4.8.

4.7. Summary

Chapter 5: working principles of electrical machines

5.1. Introduction

5.2. Physical Concepts of Torque Production

Figure 5.1a: Flux lines due to current in the stator coils.

Figure 5.1b: Flux lines due to current in the rotor conductor.

Figure 5.1c: Flux lines due to current in the stator coils and rotor conductor.

5.3. How Continuous Torque is Produced by a Motor?

Figure 5.2a: Relative angular displacement between stator and rotor magnetic field at time $t=0s$.

Figure 5.2b: Relative angular displacement between stator and rotor magnetic field at time $t=0.25s$.

Figure 5.2c: Relative angular displacement between stator and rotor magnetic field at time $t=0.5s$.

Figure 5.2d: Relative angular displacement between stator and rotor magnetic field at time $t=0.75s$.

5.4. Rotating Magnetic Field

Figure 5.3a: A simple two pole three phase stator.

Figure 5.3b: Magnetic at time instant t_1 .

Figure 5.3c: Magnetic at time instant t_2 .

Figure 5.3d: Magnetic at time instant t_3 .

5.5. Rotating Magnetic Field produced by Distributed Winding

5.5.1. Rotating Magnetic Field (4 poles) produced by a Machine Having Distributed Coils

Figure 5.4: A nine slot stator.

Figure 5.5: All the nine coils and the corresponding three phase axes.

Figure 5.6: Three phase currents.

Figure 5.7a: Axis of phase A.

Figure 5.7b: Axis of phase B.

Figure 5.7c: Axis of phase C.

Figure 5.7d: All the nine coils and the corresponding three phase axes.

Figure 5.8a: The direction of *MMF* produced by phase A winding at time instant t_1 .

Figure 5.8b: The direction of *MMF* produced by phase B winding at time instant t_1 .

Figure 5.8c: The direction of *MMF* produced by phase C winding at time instant t_1 .

Figure 5.8d: The direction of resultant *MMF* produced by phase A, B and C windings at time instant t_1 .

Figure 5.9a: The direction of *MMF* produced by phase A winding at time instant t_2 .

Figure 5.9b: The direction of *MMF* produced by phase B winding at time instant t_2 .

Figure 5.9c: The direction of *MMF* produced by phase C winding at time instant t_2 .

Figure 5.9d: The direction of the resultant *MMF* produced by all the three phases at time instant t_2 .

Figure 5.10a: The direction of *MMF* produced by phase A winding at time instant t_3 .

Figure 5.10b: The direction of *MMF* produced by phase B winding at time instant t_3 .

Figure 5.10c: The direction of *MMF* produced by phase C winding at time instant t_3 .

Figure 5.10d: The direction of resultant *MMF* produced by the three phases at time instant t_3 .

Figure 5.11a: The direction of *MMF* produced by phase A winding at time instant t_4 .

Figure 5.11b: The direction of *MMF* produced by phase B winding at time instant t_4 .

Figure 5.11c: The direction of *MMF* produced by phase C winding at time instant t_4 .

Figure 5.11d: The direction of resultant *MMF* produced by the three phases at time instant t_4 .

Figure 5.12a: The direction of *MMF* produced by phase A winding at time instant t_5 .

Figure 5.12b: The direction of *MMF* produced by phase B winding at time instant t_5 .

Figure 5.12c: The direction of *MMF* produced by phase C winding at time instant t_5 .

Figure 5.12d: The direction of resultant *MMF* produced by the three phases at time instant t_5 .

Figure 5.13a: The direction of *MMF* produced by phase A winding at time instant t_6 .

Figure 5.13b: The direction of *MMF* produced by phase B winding at time instant t_6 .

Figure 5.13c: The direction of MMF produced by phase C winding at time instant t_6 .

Figure 5.13d: The direction of resultant MMF produced by the three phases at time instant t_6 .

Animation 5.1: The direction of magnetic field produced by coils of phase A.

Animation 5.2: The direction of magnetic field produced by coils of phase B.

Animation 5.3: The direction of magnetic field produced by coils of phase C.

Animation 5.4: The direction of resultant magnetic field produced by all the three phases.

Animation 5.5: The direction of magnetic field produced by each phase and all phases taken together.

5.5.2. Rotating Magnetic Field (4 poles) produced by a Machine Having Distributed Coils

Figure 5.14: Winding scheme of a 12 slot stator that produces four poles.

Figure 5.15a: The direction of resultant MMF produced by current in phase A at time instant t_1 .

Figure 5.15b: The direction of resultant MMF produced by current in phase B at time instant t_1 .

Figure 5.15c: The direction of resultant MMF produced by current in phase C at time instant t_1 .

Figure 5.15d: The direction of resultant MMF produced by current in all the three phases at time instant t_1 .

Figure 5.15e: The flux lines due to currents in all the three phases at time instant t_1 .

Animation 5.6: The direction of magnetic field produced by coils of phase A in a four pole machine.

Animation 5.7: The direction of magnetic field produced by coils of phase B in a four pole machine.

Animation 5.8: The direction of magnetic field produced by coils of phase C in a four pole machine.

Animation 5.9: The direction of magnetic field produced by coils of three phases and their resultant flux.

Figure 5.16a: The direction of resultant MMF produced by current in phase A at time instant t_2 .

Figure 5.16b: The direction of resultant MMF produced by current in phase B at time instant t_2 .

Figure 5.16c: The direction of resultant MMF produced by current in phase C at time instant t_2 .

Figure 5.16d: The direction of resultant *MMF* produced by current in all the three phases at time instant t_2 .

Figure 5.16e: The flux lines due to currents in all the three phases at time instant t_2 .

Figure 5.17a: The direction of resultant *MMF* produced by current in phase A at time instant t_3 .

Figure 5.17b: The direction of resultant *MMF* produced by current in phase B at time instant t_3 .

Figure 5.17c: The direction of resultant *MMF* produced by current in phase C at time instant t_3 .

Figure 5.17d: The direction of resultant *MMF* produced by current in all the three phases at time instant t_3 .

Figure 5.17e: The flux lines due to currents in all the three phases at time instant t_3 .

Figure 5.18a: The direction of resultant *MMF* produced by current in phase A at time instant t_4 .

Figure 5.18b: The direction of resultant *MMF* produced by current in phase B at time instant t_4 .

Figure 5.18c: The direction of resultant *MMF* produced by current in phase C at time instant t_4 .

Figure 5.18d: The direction of resultant *MMF* produced by current in all the three phases at time instant t_4 .

Figure 5.18e: The flux lines due to currents in all the three phases at time instant t_4 .

Figure 5.19a: The direction of resultant *MMF* produced by current in phase A at time instant t_5 .

Figure 5.19b: The direction of resultant *MMF* produced by current in phase B at time instant t_5 .

Figure 5.19c: The direction of resultant *MMF* produced by current in phase C at time instant t_5 .

Figure 5.19d: The direction of resultant *MMF* produced by current in all the three phases at time instant t_5 .

Figure 5.19e: The flux lines due to currents in all the three phases at time instant t_5 .

Figure 5.20a: The direction of resultant *MMF* produced by current in phase A at time instant t_6 .

Figure 5.20b: The direction of resultant *MMF* produced by current in phase B at time instant t_6 .

Figure 5.20c: The direction of resultant *MMF* produced by current in phase C at time instant t_6 .

Figure 5.20d: The direction of resultant MMF produced by current in all the three phases at time instant t_6 .

Figure 5.20e: The flux lines due to currents in all the three phases at time instant t_6 .

Box 5.1

Figure 5.B1.1: Winding scheme of a 12 slot stator that produces four poles.

Figure 5.B1.2a: Hall effect sensor and only coil 1 of phase A is excited.

Figure 5.B1.2b: Flux density in the air gap periphery when coil 1 of phase A is excited.

Figure 5.B1.3a: Hall effect sensor and only coil 2 of phase A is excited.

Figure 5.B1.3b: Flux density in the air gap periphery when coil 2 of phase A is excited.

Figure 5.B1.4a: Hall effect sensor and only coil 3 of phase A is excited.

Figure 5.B1.4b: Flux density in the air gap periphery when coil 3 of phase A is excited.

Figure 5.B1.5a: Hall effect sensor and only coil 4 of phase A is excited.

Figure 5.B1.5b: Flux density in the air gap periphery when coil 4 of phase A is excited.

Figure 5.B1.6: Magnetic flux density in the air gap due to the current in all the coils of phase A at time instant t_1 .

Figure 5.B1.7: Magnetic flux density in the air gap due to the current in all the coils of phase B at time instant t_1 .

Figure 5.B1.8: Magnetic flux density in the air gap due to the current in all the coils of phase C at time instant t_1 .

Figure 5.B1.9: Magnetic flux density in the air gap due to all the three phases at time instant t_1 .

Figure 5.B1.10: Resultant magnetic flux density in the air gap due to all the three phases at time instant t_1 .

Figure 5.B1.11: Magnetic flux density in the air gap due to all the three phases at time instant t_2 .

Figure 5.B1.12: Resultant magnetic flux density in the air gap due to all the three phases at time instant t_2 .

Figure 5.B1.13: Magnetic flux density in the air gap due to all the three phases at time instant t_3 .

Figure 5.B1.14: Magnetic flux density in the air gap due to all the three phases at time instant t_4 .

Figure 5.B1.15: Magnetic flux density in the air gap due to all the three phases at time instant t_5 .

Figure 5.B1.16: Magnetic flux density in the air gap due to all the three phases at time instant t_6 .

Figure 5.B1.17: Resultant flux density in the air gap at time instant t_3 .

Figure 5.B1.18: Resultant flux density in the air gap at time instant t_4 .

Figure 5.B1.19: Resultant flux density in the air gap at time instant t_5 .

Figure 5.B1.20: Resultant flux density in the air gap at time instant t_6 .

Figure 5.B1.21: The resultant flux density in the air gap at different instants of time.

5.6. How to Create the Second Magnetic Field?

5.6.1. Synchronous Machines

Figure 5.21: A simple salient pole synchronous machine. The coils on the rotor carry direct current and produce the magnetic field.

5.6.2. Permanent Magnet Synchronous Machines (PMSM)

Figure 5.22: A permanent magnet synchronous machine. The two permanent magnets on the rotor produce the magnetic field.

5.6.3. Induction Machine (IM)

5.7. Why Should the Number of Poles on Stator Equal to the Number of Poles on Rotor?

Figure 5.23: A 2 pole stator and 4 pole rotor configuration.

5.8. Electrical and Mechanical Angle

Figure 5.24: A simple salient pole synchronous machine. The stator has saliency and rotor is cylindrical. The stator coils are excited by current source and as rotor moves an *EMF* is induced in the rotor coil.

Figure 5.25: Induced *EMF* in the rotor (at a constant speed of rotation) as function of rotor position.

Animation 5.10: Flux linked by rotor coil in a two pole machine.

Animation 5.11: *EMF* induced in the rotor coil of a two pole machine.

Figure 5.26: Stator with four salient poles. The direct current in the stator coils produces four poles.

Figure 5.27: Induced *EMF* in the rotor (at a constant speed of rotation) as function of rotor position. In one complete rotation of rotor (that is 360degrees), two cycles of *EMF* is induced.

Animation 5.12: *EMF* induced in the rotor coil of a four pole machine.

5.9. Summary

Chapter 6: Fundamentals of Induction Machine

6.1. Introduction

6.2. Fluxes and MMF in Induction Motor

6.2.1. Fluxes and MMF in 2 Pole Cage Rotor Induction Motor

Figure 6.1: A cage rotor induction motor with 12 slot stator and 16 slot rotor.

Figure 6.2: Stator winding scheme to produce two poles.

Animation 6.1: Construction of a 3-phase Induction Motor.

Animation 6.2: Flux lines in a two pole machine.

Figure 6.3a: Flux lines due to stator currents at time instant t_1 .

Figure 6.3b: Magnetic flux density in the air gap as measure by the Hall effect sensor at time instant t_1 .

Animation 6.3: Air gap field distribution in a two pole machine at time instant t_1 .

Figure 6.4a: Flux lines due to stator currents at time instant t_2 .

Figure 6.4b: Magnetic flux density in the air gap as measure by the Hall effect sensor at time instant t_2 .

Animation 6.4: Air gap field distribution in a two pole machine at time instant t_2 .

Figure 6.5a: Flux lines due to stator currents at time instant t_3 .

Figure 6.5b: Magnetic flux density in the air gap as measure by the Hall effect sensor at time instant t_3 .

Animation 6.5: Air gap field distribution in a two pole machine at time instant t_3 .

Figure 6.6a: Flux lines due to stator currents at time instant t_4 .

Figure 6.6b: Magnetic flux density in the air gap as measure by the Hall effect sensor at time instant t_4 .

Animation 6.6: Air gap field distribution in a two pole machine at time instant t_4 .

Figure 6.7a: Flux linked by rotor bars at time instant t_1 .

Figure 6.7b: Flux linked by rotor bars at time instant t_2 .

Figure 6.7c: Flux linked by rotor bars at time instant t_3 .

Figure 6.7d: Flux linked by rotor bars at time instant t_4 .

Figure 6.8a: Induced EMF in the rotor bar at time instant t_1 .

Figure 6.8b: Induced EMF in the rotor bar at time instant t_2 .

Animation 6.7: Flux enclosing the bar of rotors.

Figure 6.8c: Induced EMF in the rotor bar at time instant t_3 .

Figure 6.8d: Induced EMF in the rotor bar at time instant t_4 .

Animation 6.8: Induced E.M.F. in the bars of the rotor.

Figure 6.9a: Current in the rotor bars at time instant t_1 .

Figure 6.9b: Current in the rotor bars at time instant t_2 .

Figure 6.9c: Current in the rotor bars at time instant t_3 .

Figure 6.9d: Current in the rotor bars at time instant t_4 .

Animation 6.9: Current distribution in the bars of the rotor.

Box 6.1

Figure 6.B1.1a: Direction of bar current at time instant t_1 .

Figure 6.B1.1b: Direction of bar current at time instant t_2 .

Figure 6.B1.1c: Direction of bar current at time instant t_3 .

Figure 6.B1.1d: Direction of bar current at time instant t_4 .

Figure 6.10a: Magnetic field created by current in the rotor bars at time instant t_1 .

Figure 6.10b: Magnetic field created by current in the rotor bars at time instant t_2 .

Figure 6.10c: Magnetic field created by current in the rotor bars at time instant t_3 .

Figure 6.10d: Magnetic field created by current in the rotor bars at time instant t_4 .

Figure 6.11a: Direction of torque acting on rotor due to the interaction between stator and rotor magnetic fields at time instant t_1 .

Figure 6.11b: Direction of torque acting on rotor due to the interaction between stator and rotor magnetic fields at time instant t_2 .

Figure 6.11c: Direction of torque acting on rotor due to the interaction between stator and rotor magnetic fields at time instant t_3 .

Figure 6.11d: Direction of torque acting on rotor due to the interaction between stator and rotor magnetic fields at time instant t_4 .

Animation 6.10: Air gap field, Flux linkage, induced E.M.F. and bar currents without taking rotor inductance in the account.

Figure 6.12: The phasor diagram of a cage rotor induction with rotor inductance neglected.

Figure 6.13: Induced *EMF* in the rotor bars with rotor inductance taken into account.

Figure 6.14: The current in the rotor bars with rotor inductance taken into account.

Figure 6.15: The phasor diagram of a cage rotor induction with rotor inductance taken into account.

Animation 6.11: Air gap field, Flux linkage, induced E.M.F. and bar currents with taking rotor inductance in the account.

6.2.2. Fluxes and MMF in 4 Pole Cage Induction Motor

Figure 6.16: A four pole cage rotor induction motor with its winding scheme for stator.

Animation 6.12: Flux lines in a four pole machine.

Figure 6.17a: Flux lines due to balanced three phase current in the stator windings at time instant t_1 .

Figure 6.17b: Magnetic flux density along the periphery of the air gap.

Animation 6.13: Air gap field distribution in a four pole machine at time instant t_1 .

Figure 6.18: Flux lines due to balanced three phase current in the stator windings at time instant t_2 .

Figure 6.19: Flux lines due to balanced three phase current in the stator windings at time instant t_3 .

Figure 6.20: Flux lines due to balanced three phase current in the stator windings at time instant t_4 .

Animation 6.14: Air gap field distribution in a four pole machine at time instant t_2 .

Animation 6.15: Air gap field distribution in a four pole machine at time instant t_3 .

Animation 6.16: Air gap field distribution in a four pole machine at time instant t_4 .

Figure 6.21a: Flux linked by rotor bars at time instant t_1 .

Figure 6.21b: Flux linked by rotor bars at time instant t_2 .

Figure 6.21c: Flux linked by rotor bars at time instant t_3 .

Figure 6.21d: Flux linked by rotor bars at time instant t_4 .

Figure 6.22a: Induced *EMF* in rotor bars at time instant t_1 .

Figure 6.22b: Induced *EMF* in rotor bars at time instant t_2 .

Figure 6.22c: Induced *EMF* in rotor bars at time instant t_3 .

Figure 6.22d: Induced *EMF* in rotor bars at time instant t_4 .

Figure 6.23a: Current in the rotor bars at time instant t_1 .

Figure 6.23b: Current in the rotor bars at time instant t_2 .

Figure 6.23c: Current in the rotor bars at time instant t_3 .

Figure 6.23d: Current in the rotor bars at time instant t_4 .

Figure 6.24a: Magnetic field due to current in the rotor bars at time instant t_1 .

Figure 6.24b: Magnetic field due to current in the rotor bars at time instant t_2 .

Figure 6.24c: Magnetic field due to current in the rotor bars at time instant t_3 .

Figure 6.24d: Magnetic field due to current in the rotor bars at time instant t_4 .

Animation 6.17: Magnetic field and current at different rotor position for a given slip.

Figure 6.25: The angular displacement between the stator and rotor magnetic fields at different time instants.

Figure 6.26a: Magnetic field due to current in the rotor bars, taking into account the rotor inductance, at time instant t_1 .

Figure 6.26b: Magnetic field due to current in the rotor bars, taking into account the rotor inductance, at time instant t_2 .

Figure 6.26c: Magnetic field due to current in the rotor bars, taking into account the rotor inductance, at time instant t_3 .

Figure 6.26d: Magnetic field due to current in the rotor bars, taking into account the rotor inductance, at time instant t_4 .

6.2.3. Fluxes and *MMF* in 2 Pole Wound Rotor Induction Motor

Figure 6.27: Cross section of a wound rotor induction motor. In this machine, the rotor has a winding similar to stator instead of bars.

Figure 6.28: The end terminals of the rotor winding and their connection to the slip rings.

Figure 6.29: Axes of three phases of rotor in a wound rotor induction motor.

Figure 6.30a: Flux linked by the three coils of phase A.

Figure 6.30b: Flux linked by the three coils of phase B.

Figure 6.30c: Flux linked by the three coils of phase C.

Figure 6.31a: The *EMF* induced in each of the three coils of phase A.

Figure 6.31b: The *EMF* induced in each of the three coils of phase B.

Figure 6.31c: The *EMF* induced in each of the three coils of phase C.

Figure 6.32: Resultant *EMF* in each phase of rotor.

Figure 6.33: Current in each phase of rotor.

Figure 6.34a: The location of the stator field at time instant t_1 .

Figure 6.34b: The location of the rotor field, due to currents in the rotor winding, at time instant t_1 .

Figure 6.35a: The location of the stator field at time instant t_2 .

Figure 6.35b: The location of the rotor field, due to currents in the rotor winding, at time instant t_2 .

Figure 6.36a: The location of the stator field at time instant t_3 .

Figure 6.36b: The location of the rotor field, due to currents in the rotor winding, at time instant t_3 .

Figure 6.37a: The location of the stator field at time instant t_4 .

Figure 6.37b: The location of the rotor field, due to currents in the rotor winding, at time instant t_4 .

Figure 6.38a: Magnetic flux lines in a four pole wound rotor induction motor at time instant t_1 .

Figure 6.38b: Magnetic flux lines in a four pole wound rotor induction motor at time instant t_2 .

Figure 6.38c: Magnetic flux lines in a four pole wound rotor induction motor at time instant t_3 .

Figure 6.38d: Magnetic flux lines in a four pole wound rotor induction motor at time instant t_4 .

Figure 6.38e: Magnetic flux lines in a four pole wound rotor induction motor at time instant t_5 .

6.3. Rotor Action

6.4. Rotor *EMF* and Equivalent Circuit

Figure 6.39: Electrical equivalent circuit of rotor.

6.5. Complete Equivalent Circuit

Figure 6.40: Electrical equivalent circuit of stator.

Figure 6.41: Per phase electrical equivalent circuit of the induction motor.

6.6. Simplification of Equivalent Circuit

Figure 6.42: Simplified per phase electrical equivalent circuit of the induction motor.

6.7. The Electromagnetic Torque-Speed Characteristics of an Induction Motor: A Physical View

Figure 6.43a: Magnitudes of stator and rotor magnetic fields at no load.

Figure 6.43b: Magnitudes of stator and rotor magnetic fields at full load.

6.7.1. Variation of B_{gap}

Figure 6.44a: Air gap field versus rotor speed.

6.7.2. Variation of B_2

Figure 6.44b: Magnetic field in the air gap due to rotor current versus speed.

6.7.3. Variation of δ

Figure 6.44c: Variation of load angle with speed.

Figure 6.44d: Typical torque versus speed of induction motor.

6.8. Thevenin's equivalent circuit

Figure 6.45: Thevenin's equivalent circuit.

Figure 6.46a: Thevenin's equivalent circuit.

Figure 6.46b: Thevenin's modified equivalent circuit.

6.8.1. Maximum Torque

Figure 6.47a: Torque versus slip curve for different values of rotor resistance.

Figure 6.47b: Torque versus slip curve for increasing values of applied voltage.

Figure 6.47c: Torque versus slip curve for increasing values of stator resistance.

Figure 6.47d: Torque versus slip curve for increasing values of stator reactance.

Figure 6.47e: Torque versus slip curve for increasing values of rotor reactance.

6.8.2. Starting Torque

6.8.3. Power versus Slip Characteristics

Figure 6.48a: Slip versus stator resistance curve.

Figure 6.48b: Slip versus rotor resistance curve.

Figure 6.48c: Slip versus stator reactance curve.

Figure 6.48d: Slip versus rotor reactance curve.

Figure 6.49a: Maximum power versus Stator resistance curve.

Figure 6.49b: Maximum power versus Rotor resistance curve.

Figure 6.49c: Maximum power versus stator reactance curve.

Figure 6.49d: Maximum power versus rotor reactance curve.

6.9. Determination of Equivalent Circuit Parameters

6.9.1. No load test on induction motors

Figure 6.50a: Equivalent circuit at no load.

6.9.2. Block rotor test on induction motors

Figure 6.50b: Equivalent circuit at blocked rotor.

6.9.3. Determination of Equivalent circuit parameters

6.10. The phasor diagram

Figure 6.51a: Phasor diagram of induction motor.

Figure 6.51b: Phasor diagram of induction machine at any speed.

6.11. Induction motor stability

Figure 6.52a: Torque versus slip characteristics of induction machine.

Figure 6.52b: Stable operation of induction machine.

Figure 6.52c: Stable operation of induction machine.

Figure 6.52d: Unstable operation of induction machine.

6.12. Induction motor Characteristics under Various Load Conditions

6.13. Starting of induction motors

6.13.1. Starting of induction motors (Impedance Starting)

Figure 6.53a: Impedance starting.

6.13.2. Starting of induction motors (Autotransformer starting)

Figure 6.53b: Autotransformer starting.

6.13.3. Starting of induction motors (Star-delta starting)

Figure 6.53c: Star Delta Starter.

6.13.4. Starting of Wound rotor induction motors

6.13.5. Starting of Wound rotor induction motors (resistance calculation)

Figure 6.54: Wound rotor motor starting.

6.14. Induction Machine as frequency converter

6.15. Summary

Chapter 7: Speed Control of Induction Motors

7.1. Introduction

7.2. Speed Control of Induction Motor (*IM*)

Figure 7.1: Equivalent circuit of *IM*.

7.3. Constant *Volts/Hz* Control

Figure 7.2: *PU* stator phase voltage vs. *pu* stator frequency.

7.4. Implementation of Constant *Volts/Hz* Control

Figure 7.3: Closed loop induction motor drive with constant *volts/Hz* control strategy.

7.5. Steady State Performance of *IM* with Constant *Volts/Hz* Control

Example 7.1

Figure 7.4: *Torque vs. Speed* Curve for Constant *volts/Hz* control of *IM*.

Figure 7.5: Constant *Torque vs. Speed* Curve for Constant *volts/Hz* control of *IM*.

Figure 7.6: *Torque vs. Speed* Curve for Constant *volts/Hz* control of *IM* at higher offset voltage.

Figure 7.7: *Power factor vs. Slip* Curve for Constant *volts/Hz* control of *IM*.

Figure 7.8: *Stator Current vs. Slip* Curve for Constant *volts/Hz* control of *IM*.

Figure 7.9: *Torque vs. Slip* Curve for Constant *volts/Hz* control of *IM*.

7.6. Summary

Chapter 8: Fundamentals of Synchronous Machines

8.1. Introduction

8.2. Excitation System for Synchronous Generators

Figure 8.1: Functional block diagram of a synchronous generator excitation control system.

Figure 8.2a: DC excitation system.

Figure 8.2b: Field-controlled alternator rectifier excitation system.

8.3. Main features of the synchronous generators

8.4. Operating principle of synchronous machine

Figure 8.3: Balanced three phase currents in the stator winding.

Figure 8.4a: Location of stator and rotor magnetic field at time instant t_1 .

Figure 8.4b: Location of stator and rotor magnetic field at time instant t_2 .

Figure 8.4c: Location of stator and rotor magnetic field at time instant t_3 .

Figure 8.4d: Location of stator and rotor magnetic field at time instant t_4 .

Figure 8.4e: Location of stator and rotor magnetic field at time instant t_5 .

Figure 8.4f: Location of stator and rotor magnetic field at time instant t_6 .

Figure 8.5a: Location of stator and rotor magnetic field at time instant t_1 .

Figure 8.5b: Location of stator and rotor magnetic field at time instant t_2 .

Figure 8.5c: Location of stator and rotor magnetic field at time instant t_3 .

Figure 8.5d: Location of stator and rotor magnetic field at time instant t_4 .

Figure 8.5e: Location of stator and rotor magnetic field at time instant t_5 .

Figure 8.5f: Location of stator and rotor magnetic field at time instant t_6 .

Figure 8.6a: Location of stator and rotor magnetic field at time instant t_1 .

Figure 8.6b: Location of stator and rotor magnetic field at time instant t_2 .

Figure 8.6c: Location of stator and rotor magnetic field at time instant t_3 .

Figure 8.6d: Location of stator and rotor magnetic field at time instant t_4 .

Figure 8.6e: Location of stator and rotor magnetic field at time instant t_5 .

Figure 8.6f: Location of stator and rotor magnetic field at time instant t_6 .

8.5.1 Cylindrical rotor synchronous machine

Figure 8.7: Distribution of the stator and rotor magnetic field along the air gap periphery at a given point of time.

Animation 8.1: Construction of a 3-phase Cylindrical rotor synchronous machine.

Figure 8.8: Induced *EMF* in three phases of the stator winding as a function of rotor position. The rotor rotates at angular speed of ωr .

Figure 8.9: A synchronous generator connected to a resistive load.

Figure 8.10a: The resultant magnetic field in synchronous machine.

Figure 8.10b: The induced *EMF* and current in phase A. Since the inductance is neglected, the induced *EMF* and the current are in phase.

Figure 8.11: The induced *EMF* and current in phase A. Since the inductance is considered, the current lags the induced *EMF*.

Figure 8.12a: A synchronous generator connected to an inductive load.

Figure 8.12b: The induced *EMF* and current in phase A. The load connected to the stator terminals is purely inductive and hence, the current lags the induced *EMF* by 90° . The stator resistance is neglected.

Figure 8.12c: Since the load across the stator terminals is purely inductive, the armature field and the rotor field oppose each other. The armature field is demagnetizing in nature.

Figure 8.13a: A synchronous generator connected to a capacitive load.

Figure 8.13b: The induced EMF and current in phase A. The load connected to the stator terminals is purely capacitive and hence, the current leads the induced EMF by 90° . The stator resistance is neglected.

Figure 8.13c: Since the load across the stator terminals is purely capacitive, the armature field and the rotor field are in same direction. The armature field is magnetizing in nature.

8.5.2 Salient rotor synchronous machine

Figure 8.14: Construction of a six pole salient pole synchronous generator.

Animation 8.2: Construction of a 3-phase Salient rotor synchronous machine.

Figure 8.15a: The magnetic field created by the stator winding is along the x-axis and the rotor poles are also aligned along x-axis. Hence, the flux lines of the stator pole face low reluctance.

Figure 8.15b: The magnetic field created by the stator winding is along the y-axis and the rotor poles are also aligned along x-axis. Hence, the flux lines of the stator pole face high reluctance.

Figure 8.16a: The armature current and induced EMF relation in case of lagging power factor load.

Figure 8.16b: The armature current and induced EMF relation in case of leading power factor load.

Box 8.1

Figure 8.B1.1: The rotor is aligned along the x-axis and the coil axis is also aligned along the x -axis.

Figure 8.B1.2: Flux linkage and EMF waveform for a complete rotation of the rotor in case the rotor field axis was initially aligned with the x -axis.

Figure 8.B1.3: The rotor is aligned along the y -axis and the coil axis is also aligned along the x -axis.

Figure 8.B1.4: Flux linkage and EMF waveform for a complete rotation of the rotor in case the rotor field axis was initially aligned with the y -axis.

8.6. Phasor diagram of a synchronous machine

Figure 8.17: The phasor diagram of a cylindrical rotor synchronous generator for a lagging power factor load.

Figure 8.18: Flux linkage and EMF waveform for a complete rotation of the rotor in case the rotor field axis was initially aligned with the y -axis.

Figure 8.19: The per phase equivalent circuit of three phase synchronous generator.

Figure 8.20a: The phasor diagram of a cylindrical rotor synchronous generator for a lagging power factor load and neglecting the drop across armature.

Figure 8.20b: The phasor diagram of a cylindrical rotor synchronous generator for a leading power factor load and neglecting the drop across armature.

8.7. Power and torque in synchronous generators

Figure 8.21: The phasor diagram of a cylindrical rotor synchronous generator for a lagging power factor load and neglecting the drop across armature. This phasor diagram is used to determine the power delivered by the generator.

Figure 8.22: Variation of power delivered by the generator as a function load angle.

8.8. Stand alone operation of synchronous generators

Figure 8.23: The phasor diagram of a cylindrical rotor synchronous generator. Here it is assumed that $\Phi_{\text{rotor}} \gg \Phi_{\text{arm}}$ and hence, $E_{\text{airgap}} \gg E_f$ and $\Phi_{\text{airgap}} \approx \Phi_{\text{rotor}}$.

Figure 8.24: The per unit equivalent circuit of a synchronous generator feeding a load.

8.8.1. Varying load with unity power factor

8.8.2. Varying load with lagging power factor

Figure 8.25b: Variation of V_t with increase in I_a for a lagging power factor load.

8.8.3. Varying load with leading power factor

Figure 8.25c: Variation of V_t with increase in I_a for a leading power factor load.

8.9. Voltage regulation of an alternator

Figure 8.26: As the load at a fixed power factor increases, the field excitation current is increased so that V_t remains constant. In this case EMF increases due to increase in field excitation current.

8.10. Compounding characteristics of the synchronous generators

Figure 8.27a: Synchronous generator phasor diagram for constant terminal voltage and feeding a lagging power factor load. In this case $E_f > 1 p.u.$

Figure 8.27b: Synchronous generator phasor diagram for constant terminal voltage and feeding a unity power factor load. In this case E_f is slightly greater than $1 p.u.$

Figure 8.27c: Synchronous generator phasor diagram for constant terminal voltage and feeding a leading power factor load. In this case $E_f > 1 p.u.$

Figure 8.28: The compounding characteristics of a synchronous generator.

8.11. Basic principle of operation of synchronous motor

Figure 8.29: Construction of synchronous motor.

8.12. Equivalent circuit of synchronous motor

Figure 8.30a: The equivalent circuit of three phase synchronous motor.

Figure 8.30b: The per phase equivalent circuit of three phase synchronous motor.

8.13. The effect of load changes on a synchronous motor

Figure 8.31a: Phasor diagram for the initial condition of the synchronous motor. The motor initially operates at a leading power factor load.

Figure 8.31b: Phasor diagram of synchronous motor depicting the increase in load on the rotor shaft.

8.14. The effect of field current on the performance of synchronous motor

Figure 8.32: Impact of increase in field excitation current on a synchronous motor fed by a constant voltage source and driving a constant load.

Figure 8.33: Synchronous motor *V* curves.

8.15. Use of synchronous motor for power factor correction

Figure 8.34: The motors fed from the infinite or the grid.

8.16. Summary

References

Abbreviations

Definitions